Assessing the liquefaction risk reduction of reinforced soils: a homogenization approach

Maxime Gueguin, Ghazi Hassen, Patrick De Buhan

ASSESSING THE LIQUEFACTION RISK REDUCTION OF REINFORCED SOILS: A HOMOGENIZATION APPROACH

Maxime Gueguin, Ghazi Hassen and Patrick de Buhan
Université Paris-Est, Laboratoire Navier (UMR 8205), CNRS, ENPC, IFSTTAR, Marne-La-Vallée, France

ABSTRACT: *In this contribution, an evaluation is given for the reduction of the liquefaction risk, which can be expected from reinforcing the soil by a periodic array of inclusions. Following a definition of the liquefaction risk reduction factor, the link is then established with the increase of longitudinal shear stiffness of the reinforced soil. Based on the homogenization theory for elastic periodic media, different geometries of the reinforcing inclusions are examined, with a particular focus on circular cylindrical (columnar) inclusions on the one hand, two mutually orthogonal arrays of trenches (cross trench configuration) on the other hand. A variational method based on minimum energy principles allows the derivation of theoretical lower and upper bounds for the reinforced soil longitudinal shear modulus. A comparison with results obtained from numerical simulations performed with a standard finite element code is then presented.*

1 INTRODUCTION

Soils reinforced by inclusions may be considered as composite materials and studied using homogenization methods. These methods are applicable considering the fact that the spacing between two neighboring columns is small in comparison with the overall dimensions of the structure. The validity of the homogenization method has been demonstrated as concerned the evaluation of the macroscopic elastic behaviour of fibre composite materials (Hashin & Rosen 1964; Hashin 1983) as well as, at a much larger scale, for soils strengthened by columnar inclusions (Balaam & Booker 1981; Canetta & Nova 1989; Abdelkrim & de Buhan 2007). Yet, the applications to geotechnical problems have been so far restricted to the evaluation of the settlement of the reinforced foundation under vertical loading and the pure shear loading problem has been rarely the subject of studies, even if it plays a major role in the response of reinforced ground subject to earthquake loading.

The present contribution intends to evaluate the liquefaction risk for a reinforced soil under a seismic solicitation, both constituents being considered as isotropic linear elastic materials with perfect bonding at their interface. First of all, a liquefaction risk reduction factor is defined, based on the analysis of the behaviour of a reinforced soil subject to a seismic wave, involving its macroscopic longitudinal shear stiffness (section 2). Two configurations will be more specifically studied. First, section 3 derives the analytical bounds for the longitudinal shear stiffness of a column-reinforced soil and the associated liquefaction risk reduction factor. Then section 4 develops the same evaluation for a cross trench reinforced soil and a comparison with the previous configuration is carried out, exhibiting a much greater efficiency in terms of liquefaction risk reduction for the cross trench configuration than for the columnar configuration.

2 SOIL REINFORCEMENT AS A LIQUEFACTION MITIGATION TECHNIQUE

2.1 Problem statement

Earthquakes induce major troubles on civil engineering structures, which may lead to major disasters. From a geotechnical point of view, one of the biggest threats is the so-called soil liquefaction phenomenon. Indeed a seismic solicitation involves a cyclic shear strain of the ground, which generates an excess pore water pressure in the different water-satured materials (sands or silts), leading to a liquefaction phenomenon, that is a collapse of their resistance. This may considerably reduce the bearing capacity of the soil.

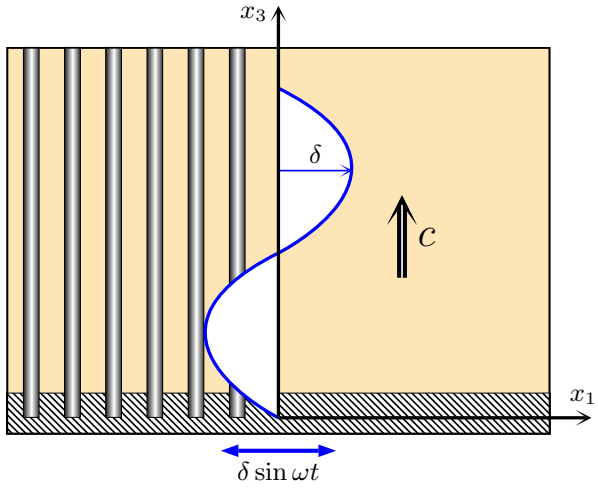

Fig. 1. Vertical propagation of a seismic shear wave in a soil layer.

The loading induced by a seismic loading can be schematized by a harmonic shear wave (see Figure 1) defined as:

$$\underline{\xi}\left(\underline{x},t\right) = \delta \sin\left[\omega\left(t - \frac{x_3}{c}\right)\right]\underline{e}_1 \tag{1}$$

where δ is the horizontal displacement amplitude and ω the angular frequency which characterize the seismic loading.

The shear wave velocity c is a characteristic of the soil and can be linked to the soil mass density ρ and the *longitudinal shear stiffness* G_L by the following classical relationship:

$$c = \sqrt{\frac{G_L}{\rho}} \tag{2}$$

where G_L is the component of the elastic stiffness tensor of the soil relating the shear stress and strain in the $(\underline{e}_1, \underline{e}_3)$ plane. For an isotropic elastic material, G_L reduces to the classical shear modulus (Lamé constant).

The cyclic strain field associated with the displacement field given by (1) is then:

$$\underline{\underline{\varepsilon}}\left(\underline{x},t\right) = -\delta\frac{\omega}{2c}\cos\left[\omega\left(t - \frac{x_3}{c}\right)\right]\left(\underline{e}_1 \otimes \underline{e}_3 + \underline{e}_3 \otimes \underline{e}_1\right) \tag{3}$$

corresponding to a pure shear strain amplitude γ equal to:

$$\gamma = \delta \frac{\omega}{2c} = \frac{\delta\omega}{2}\sqrt{\frac{\rho}{G_L}} \tag{4}$$

The accumulation of excess pore pressure, and thus the risk of liquefaction, is directly connected to this cyclic shear strain amplitude.

2.2 Shear strain amplitude localization in reinforced soils

In order to avoid any risk of liquefaction a possible solution is to strengthen the soil by the incorporation of inclusions (example of stone or vibro-concrete columns: Baez & Martin (1993) and Adalier et al. (2003)). The volume fraction occupied by the inclusion is denoted by η. One should distinguish the macroscopic shear strain amplitude γ^{hom} of the reinforced soil, seen as a homogenized material, and the average of the amplitude $\langle\gamma\rangle_s$ in the original soil in the presence of reinforcement.

An isotropic non-reinforced soil with a shear stiffness denoted by G_s is first compared to a reinforced soil, the macroscopic longitudinal shear stiffness of which is denoted by G_L. The ratio between the shear strain amplitude of these two materials subject to the same shear wave (1) (γ_s and γ^{hom} respectively) is deduced from (4):

$$\frac{\gamma^{hom}}{\gamma_s} = \sqrt{\frac{G_s}{G_L}} \tag{5}$$

with the simplifying assumption that the original soil mass density ρ_s is almost equal to the reinforced soil mass density $\langle\rho\rangle = (1-\eta)\rho_s + \eta\rho_r$. It is clear that this ratio is less than or equal to one, since the reinforcement strengthens the original soil. The amplitude of the homogenized soil shear strain is then smaller than that of the original soil (see Fig. 2).

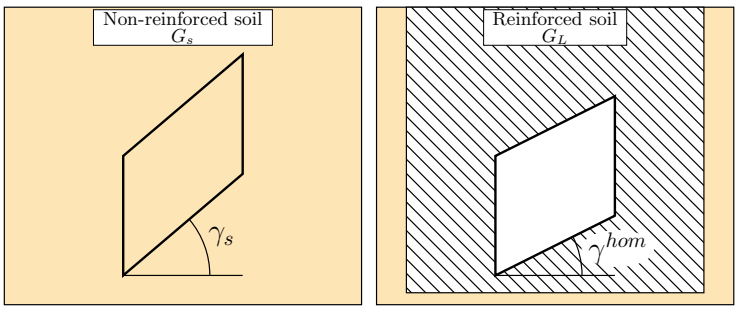

Fig. 2. Shear strain amplitude: (a) case of non-reinforced soil, (b) case of reinforced soil.

In fact, the relevant comparison is to be made between γ_s and the average value of the shear strain $\langle\gamma\rangle_s$ in the soil in the presence of reinforcement (see Figure 3), defined as:

$$\underline{\underline{\epsilon}} = \gamma^{hom}\left(\underline{e}_1 \otimes \underline{e}_3 + \underline{e}_3 \otimes \underline{e}_1\right) \;\rightarrow\; \langle\gamma\rangle_s = \frac{1}{\mathcal{C}_s}\int_{\mathcal{C}_s} \varepsilon_{13}\, dV = \lambda\gamma^{hom} \tag{6}$$

where $\mathcal{C}_s$ denotes the domain occupied by the soil and λ is defined as a *localization factor*. Its value depends on the geometry of the inclusions as it will be seen in the following sections, but will be greater than unity, the original soil having a smaller stiffness G_s than reinforcement material denoted by G_r.

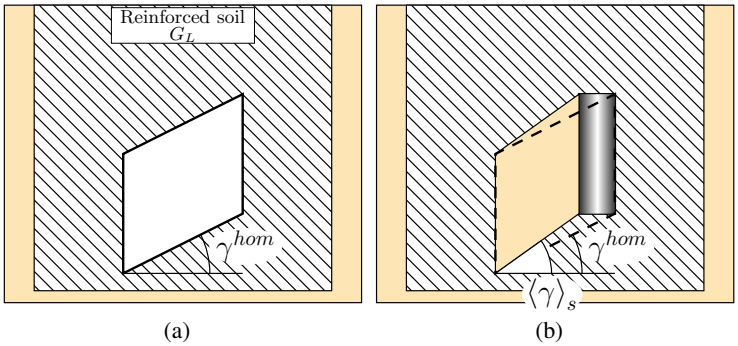

Fig. 3. Shear strain amplitude: (a) case of reinforced soil see as a homogenized material, (b) decomposition in both constituants.

The reduction of potential risk of soil liquefaction to be expected from the stiffening of the reinforcement by inclusions, which will conventionally be called *risk reduction factor* R, is defined as:

$$R = \frac{\langle\gamma\rangle_s}{\gamma_s} = \lambda\sqrt{\frac{G_s}{G_L}} \tag{7}$$

This factor, to be compared to unity, expresses the competition between the strenghtening effect and the localization in the soil. An evaluation of R will be now performed for different geometries of reinforcement.

3 LONGITUDINAL SHEAR MODULUS AND RISK REDUCTION FACTOR OF COLUMN-REINFORCED SOIL

The first case investigated is a group of circular cylindrical columnar inclusions introduced in a soil with a volume fraction $\eta = \pi\rho^2$, where ρ is the radius of a column, assuming that the side of the unit cell is taken equal to unity (Figure 4).

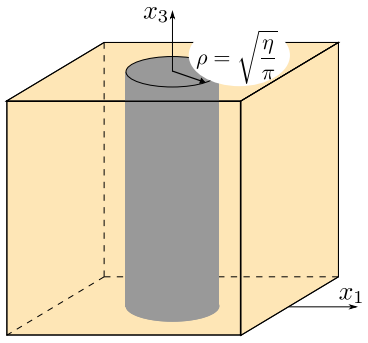

Fig. 4. Unit cell for a column configuration of reinforcement.

3.1 Upper bound estimate for G_L

It can proved (Gueguin et al. 2013) that, for any macroscopic strain $\underline{\underline{\epsilon}}$ and any displacement field $\underline{\xi}'$ kinematically admissible with $\underline{\underline{\epsilon}}$, the *minimum principle of the potential energy* gives the following inequality:

$$\forall \underline{\underline{\epsilon}},\ \forall \underline{\xi}' \text{ k.a. with } \underline{\underline{\epsilon}}, \quad \frac{1}{2}\underline{\underline{\epsilon}} : \mathbf{c}^{hom} : \underline{\underline{\epsilon}} \leq \left\langle \frac{1}{2}\underline{\underline{\varepsilon}}'(\underline{x}) : \mathbf{c}(\underline{x}) : \underline{\underline{\varepsilon}}'(\underline{x}) \right\rangle \tag{8}$$

where $\mathbf{c}(\underline{x})$ denotes the fourth order tensor of elastic moduli at point $\underline{x}$ of the unit cell and $\mathbf{c}^{hom}$ represents the macroscopic elastic stiffness tensor.

The prescribed macroscopic strain $\underline{\underline{\epsilon}}$ being of the form:

$$\underline{\underline{\epsilon}} = \Gamma \left(\underline{e}_1 \otimes \underline{e}_3 + \underline{e}_3 \otimes \underline{e}_1 \right) \tag{9}$$

it follows that for this particular shear strain the left member of (8) simplifies to:

$$\frac{1}{2}\underline{\underline{\epsilon}} : \mathbf{c}^{hom} : \underline{\underline{\epsilon}} = 2G_L\Gamma^2 \tag{10}$$

so that we obtain an upper bound value for the macroscopic longitudinal shear modulus:

$$\forall \underline{\xi}' \text{ k.a. with } \underline{\underline{\epsilon}} = \Gamma \left(\underline{e}_1 \otimes \underline{e}_3 + \underline{e}_3 \otimes \underline{e}_1 \right), \quad G_L \leq \frac{\left\langle \underline{\underline{\varepsilon}}'(\underline{x}) : \mathbf{c}(\underline{x}) : \underline{\underline{\varepsilon}}'(\underline{x}) \right\rangle}{4\Gamma^2} \tag{11}$$

For an adequate displacement field $\underline{\xi}'$, it can be proved that the upper bound is expressed as:

$$G_L \leq G_{L,col}^{ub} = G_s \left[1 + \frac{2\eta \left(G_r - G_s \right)}{\left(G_r + G_s \right) - \frac{4\eta}{\pi} \left(G_r - G_s \right)} \right] \tag{12}$$

3.2 Lower bound estimate for G_L

Using the *minimum principle of the complementary energy* with a macroscopic stress $\underline{\underline{\Sigma}}$ as loading parameter, a lower bound can be found for the same problem. For any stress field $\underline{\underline{\sigma}}'$ statically admissible with $\underline{\underline{\Sigma}}$, this principle may be written as:

$$\forall \underline{\underline{\Sigma}},\ \forall \underline{\underline{\sigma}}' \text{ s.a. with } \underline{\underline{\Sigma}}, \quad \frac{1}{2}\underline{\underline{\Sigma}} : \mathbf{s}^{hom} : \underline{\underline{\Sigma}} \leq \left\langle \frac{1}{2}\underline{\underline{\sigma}}'(\underline{x}) : \mathbf{s}(\underline{x}) : \underline{\underline{\sigma}}'(\underline{x}) \right\rangle \tag{13}$$

where $\mathbf{s}^{hom} = \left(\mathbf{c}^{hom} \right)^{-1}$ and $\mathbf{s}(\underline{x}) = \left(\mathbf{c}(\underline{x}) \right)^{-1}$ are the macroscopic and local elastic compliance tensors, respectively.

For a macroscopic pure shear stress $\underline{\underline{\Sigma}}$ of the form:

$$\underline{\underline{\Sigma}} = T \left(\underline{e}_1 \otimes \underline{e}_3 + \underline{e}_3 \otimes \underline{e}_1 \right) \tag{14}$$

the inequality (13) gives:

$$\forall \underline{\underline{\sigma}}' \text{ s.a. with } \underline{\underline{\Sigma}} = T \left(\underline{e}_1 \otimes \underline{e}_3 + \underline{e}_3 \otimes \underline{e}_1 \right), \quad \frac{T^2}{2G_L} \leq \left\langle \frac{1}{2}\underline{\underline{\sigma}}'(\underline{x}) : \mathbf{s}(\underline{x}) : \underline{\underline{\sigma}}'(\underline{x}) \right\rangle \tag{15}$$

As a result, for an appropriately selected stress field (Gueguin et al. 2013), a lower bound for the longitudinal shear modulus of a column reinforced soil may be written as:

$$G_L \geq G_{L,col}^{lb} = G_s \left[1 - \frac{2\eta \left(G_r - G_s \right)}{\left(G_r + G_s \right) + \frac{4\eta}{\pi} \left(G_r - G_s \right)} \right]^{-1} \tag{16}$$

3.3 Comparison with numerical results for R

Two different estimates R_{col}^{+} and R_{col}^{-} of the risk reduction factor can be obtained from the displacement and stress fields previously used for deriving the bounds of G_L. Both are represented in Figure 6 as functions of the reinforcement volume fraction. After calculations, the first risk reduction factor estimate obtained from the displacement field is:

$$R_{col}^{+} = \lambda_{col}^{+} \sqrt{\frac{G_s}{G_{L,col}^{ub}}} \tag{17}$$

with

$$\lambda_{col}^{+} = \frac{1}{1-\eta} \left(1 - \frac{2\eta}{\left(1 + \frac{G_r}{G_s} \right) + \frac{4\eta}{\pi} \left(1 - \frac{G_r}{G_s} \right)} \right) \tag{18}$$

The second risk reduction factor estimate derives from the stress field used for deriving the lower bound of G_L and can be expressed as:

$$R_{col}^{-} = \lambda_{col}^{-} \sqrt{\frac{G_s}{G_{L,col}^{lb}}} \tag{19}$$

where

$$\lambda_{col}^{-} = \frac{G_{L,col}^{lb}}{G_s} \frac{1}{1-\eta} \left(1 - \frac{2\eta \frac{G_r}{G_s}}{\left(1 + \frac{G_r}{G_s} \right) - \frac{4\eta}{\pi} \left(1 - \frac{G_r}{G_s} \right)} \right) \tag{20}$$

R_{col}^{+} and R_{col}^{-} can also be compared with numerical simulations performed with the standard finite element code Cast3M (2003). Owing to the symmetries of geometry and loading, it can be proved that calculations may be done on a "slice" of the half unit cell. For this comparison, typical values of material parameters are adopted, namely a shear stiffness ratio between the column and the soil $\frac{G_r}{G_s}$ equal to 10 and a reinforcement volume fraction varying from $\eta = 0\%$ to $\eta = 40\%$. An exaggerated deformed configuration of the reinforced soil is sketched in Figure 5 (with $\eta = 12.6\%$) and an evaluation of R is numerically performed under shear loading.

It can be seen from Figure 6 that the two estimates R_{col}^{+} (plain curve) and R_{col}^{-} (dashed curve) bracket the numerical values (square symbols) even though they cannot be rigorously interpreted as bounds on R. It is worth noting that their average value (dashdotted curve) is a very accurate estimate for the reduction factor, numerical and analytical estimates show that column reinforcement technique is almost useless in terms of risk liquefaction reduction. Indeed the different

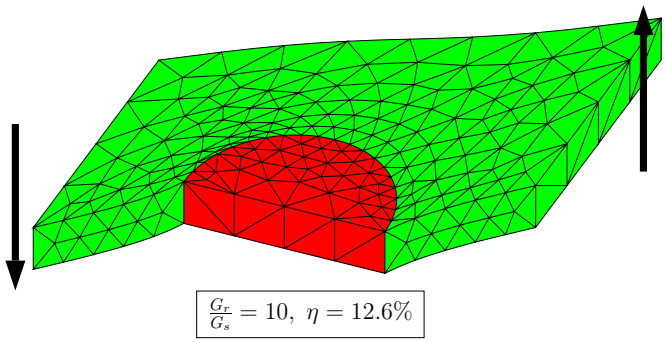

Fig. 5. Deformed configuration of a column reinforced soil under longitudinal shear loading (f.e.m calculation).

estimates of R being greater than unity, a slight increase in risk may be even observed for a column reinforced soil.

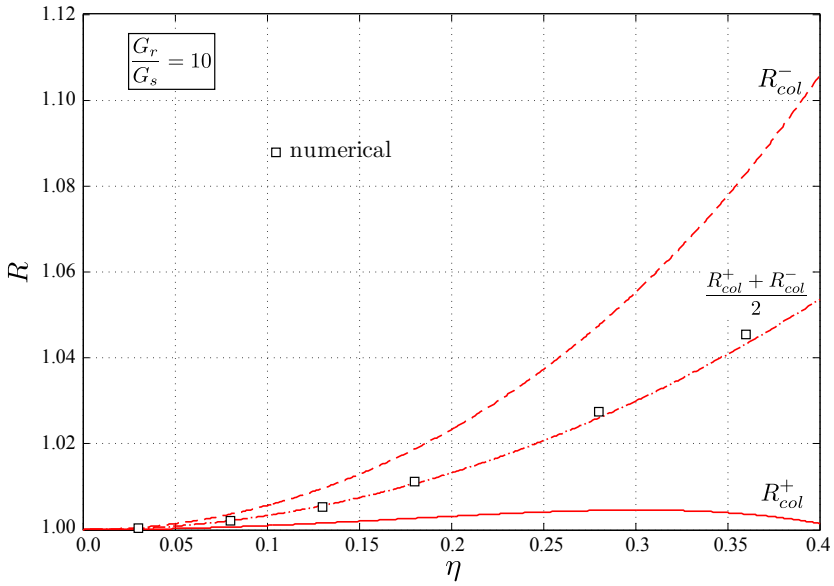

Fig. 6. Evaluations of the liquefaction risk reduction factor for a column reinforced soil.

4 THE CASE OF CROSS TRENCH CONFIGURATION

Performance of the most frequently used configuration of reinforcement by columnar inclusions being poor, a potentially innovative reinforcement technique (which is beginning to develop in practice) consists in improving the soil by a network of two perpendicular arrays of trenches, forming a ”honeycomb structure” embedded in the soil. This geometry is sketched in Figure 7 and will be called *cross trench* configuration. The thickness of a trench is noted t and the side of the unit cell is taken equal to unity so that the reinforcement volume fraction is $\eta = t(2 - t)$.

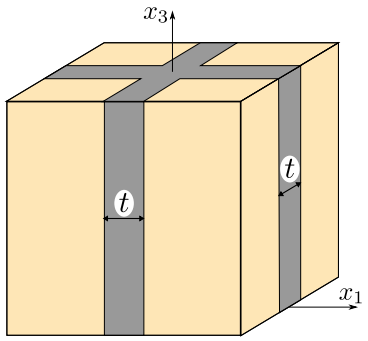

Fig. 7. Unit cell for a cross trench configuration of reinforcement.

4.1 Bounds and numerical estimates

Both variationnal methods already used for the column reinforced soil are implemented for the cross trench reinforcement configuration. On the basis of analytical calculations developed by Gueguin et al. (2013), it can be established that a first estimate of the risk reduction factor deduced from (8) is:

$$R_{ct}^{+} = \lambda_{ct}^{+} \sqrt{\frac{G_s}{G_{L,ct}^{ub}}} \tag{21}$$

with

$$G_{L,ct}^{ub} = G_r \left[\frac{\sqrt{1-\eta} + \frac{G_r}{G_s}\left(1-\sqrt{1-\eta}\right)}{\left(\eta - 1 + \sqrt{1-\eta}\right) + \frac{G_r}{G_s}\left(2-\eta-\sqrt{1-\eta}\right)} \right] \tag{22}$$

and

$$\lambda_{ct}^{+} = \left(2 - \eta - \sqrt{1-\eta} + \frac{G_s}{G_r}\left(\eta - 1 + \sqrt{1-\eta}\right) \right)^{-1} \tag{23}$$

Using (13) with an appropriate stress field, a second estimate of the risk reduction factor of a cross trench reinforced soil can be written as:

$$R_{ct}^{-} = \lambda_{ct}^{-} \sqrt{\frac{G_s}{G_{L,ct}^{lb}}} \tag{24}$$

with

$$G_{L,ct}^{lb} = G_s \left[\frac{1-\eta}{(1-\eta) + \frac{G_s}{G_r}\left(\sqrt{1-\eta} - (1-\eta)\right)} + \frac{G_r}{G_s}\left(1-\sqrt{1-\eta}\right) \right] \tag{25}$$

and

$$\lambda_{ct}^{-} = \left(\sqrt{1-\eta} + \frac{G_s}{G_r}\left(1-\sqrt{1-\eta}\right) \right)^{-1} \tag{26}$$

A numerical simulation can also be made for this configuration and results are compared to both previous estimates of R. Figure 8 illustrates the fact that the reinforcing trench placed in the loading plane fully contributes to the reinforced shear stiffness, while the other trench perpendicular to the loading plane undergoes much less deformation. The cross trench reinforcement

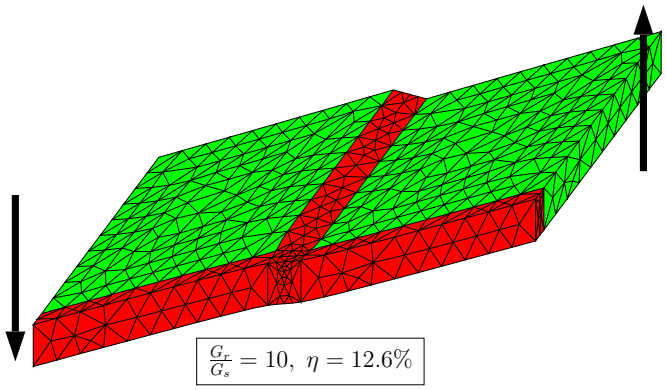

Fig. 8. Deformed configuration of a cross trench reinforced soil under longitudinal shear loading.

provides a kind of "bracing effect" to the shear loading.

Figure 9 displays the comparison between these estimates of R for a cross trench reinforced soil. A first remark is that the average value of R_{ct}^{+} and R_{ct}^{-} provides an excellent evaluation of this risk reduction factor. It is also worth noting that R is decreasing when η increases and is always less than unity. The efficience of the cross trench reinforcement is highlighted here, the risk being reduced by 24% for $\eta = 20\%$.

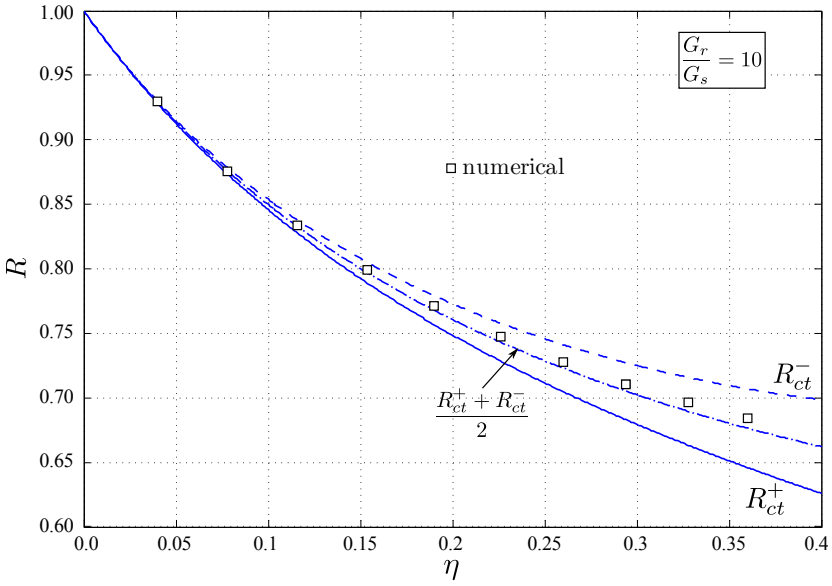

Fig. 9. Evaluations of the liquefaction risk reduction factor for a cross trench reinforced soil.

4.2 Parametric study for the risk reduction factor

The shear stiffness ratio $\frac{G_r}{G_s}$ and the reinforcement volume fraction η mainly influence the performance of the reinforcement technique in terms of liquefaction risk. For the cross trench configuration, a study has been made, choosing some fixed values of one parameter and expressing R as function of the other (see Figures 10 and 11). For the sake of clarity, only the average value

of the two estimates of this risk reduction factor are represented.

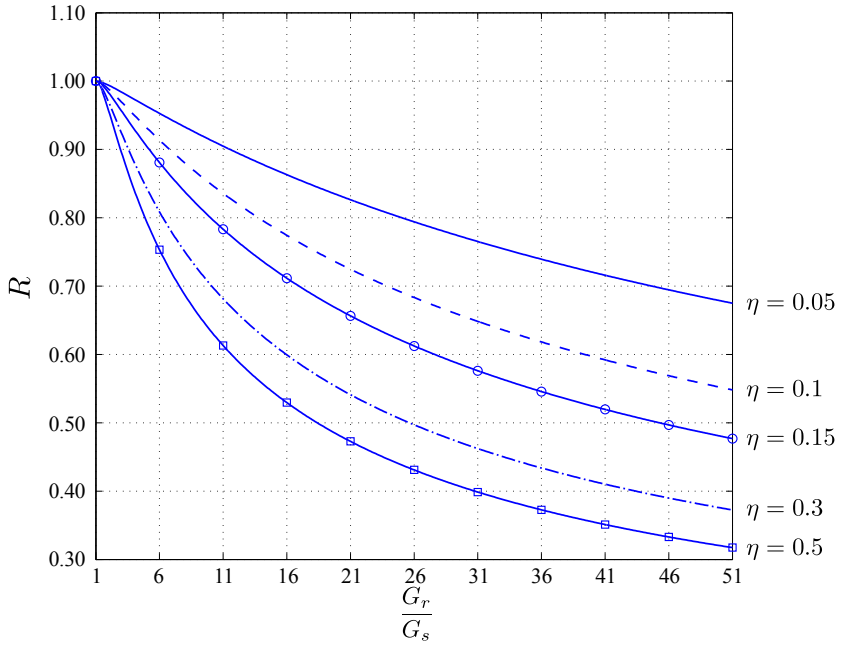

Fig. 10. Risk reduction factor of cross trench configuration as function of shear stiffness ratio $\frac{G_r}{G_s}$ for fixed values of η.

For different fixed values of η, the beneficial effect of the reinforcement is highlighted in Figure 10. However, it is worth noting that, for a shear stiffness ratio equal to 50, the risk reduction factor decreases from 0.68 to 0.48 when η goes from 5% to 15% while its decreases from 0.48 to 0.32 when η goes from 15% to 50%. This suggests that there is no need to increase the thickness of the trenches indefinitely, since the gain in terms of liquefaction risk being alternated.

In the same way, for different fixed values of $\frac{G_r}{G_s}$, the need to increase η is more obvious for small shear stiffness ratio. Indeed, for $\frac{G_r}{G_s} = 50$, the risk reduction factor rapidly decreases for small volume reinforcement fraction, then much more smoothly for higher volume fractions (Fig. 11).

5 CONCLUSIONS

Using the homogenization method for elastic periodic media, it has been possible to produce different estimates for the liquefaction risk reduction factor for a column reinforced soil as well as for a cross trench configuration. Analytical calculations allow to bracket the longitudinal shear stiffness for both techniques of reinforcement. An interesting result is that the reinforcement by columnar inclusions doesn't reduce the liquefaction risk, whereas the cross trench configuration provides an accurate reduction of this risk.

A short parametric study has been developed here for the cross trench reinforced soil depending on the two material and geometrical key parameters, namely the reinforcement volume fraction and the shear modulus ratio. All estimates being given by analytical formulas, charts may be easily drawn for different values of those characteristics which could be highly usefull

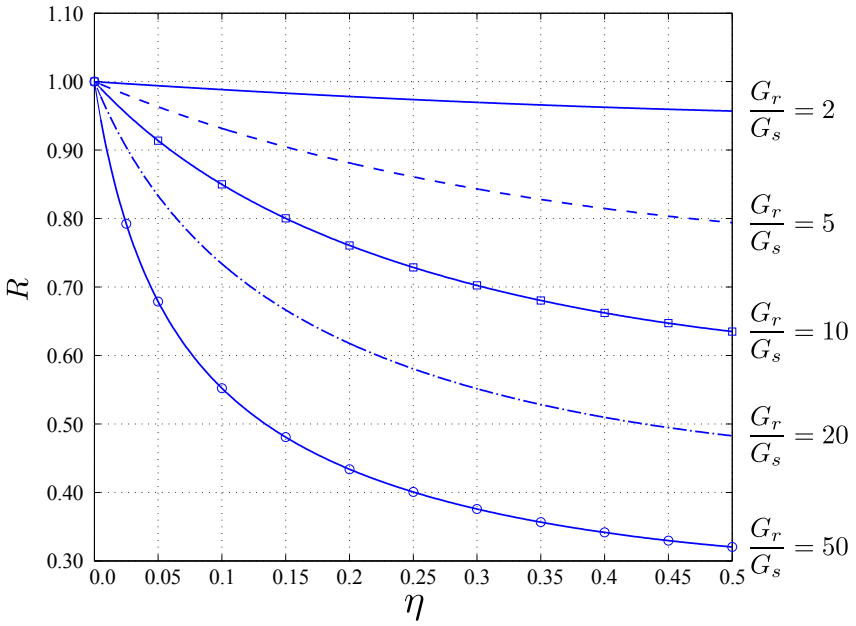

Fig. 11. Risk reduction factor of cross trench configuration as function of η for fixed values of $\frac{G_r}{G_s}$.

from an engineering design viewpoint. These results provide a strong theoretical background to the development of the cross trench reinforcement technique.

REFERENCES

Abdelkrim, M. & de Buhan, P. (2007). An elastoplastic homogenization procedure for predicting the settlement of a foundation reinforced by columns. *European J. of Mechanics, A/Solids 26*, 736–757.

Adalier, K., Elgamal, A., Meneses, J., & Baez, J. (2003). Stone columns as liquefaction countermeasure in non plastic silty soils. *Soil Dyn. Earthquake Eng. 23*, 571–584.

Baez, J. & Martin, G. (1993). Advances in the design of vibro systems for the improvement of liquefaction resistance. In *Proc. Symp. Ground improvement*, Canada, pp. 1–16. Vancouver Geotechnical Society.

Balaam, N. & Booker, J. (1981). Analysis of rigid rafts supported by granular piles. *Int. J. Num. Anal. Meth. Geomech. 5*, 379–403.

Canetta, G. & Nova, R. (1989). A numerical method for the analysis of ground improved by columnar inclusions. *Comput. Geotech. 7*, 99–114.

Cast3M (2003). http://www-cast3m.cea.fr.

Gueguin, M., de Buhan, P., & Hassen, G. (2013). A homogenization approach for evaluationg the longitudinal shear stiffness of reinforced soils: columns *vs*. cross trench configuration. *Int. J. Num. Anal. Meth. Geomech.*, Accepted for publication.

Hashin, Z. (1983). Analysis of composite materials-a survey. *J. Appl. Mech. 50*, 481–505.

Hashin, Z. & Rosen, B. (1964). The elastic moduli of fiber-reinforced materials. *J. Appl. Mech. 21*, 233–242.